DAVID E. IRVINE

EXTREME WAVES IN THE AGULHAS—A CASE STUDY IN WAVE-CURRENT INTERACTION

Analysis of a simple model of swell encountering a current shows the interaction to be highly sensitive to the curvature of the current. This points to a possible mechanism for the generation of extreme waves.

THE SUBTLE CLASSICAL ADVANTAGE

The study of ocean waves is essentially a branch of classical physics. Simple forms of mass, momentum, and energy conservation are frequently sufficient to describe the relevant governing laws. The mathematical representation of waves is straightforward; they often can be adequately described as moderate undulations in an otherwise undisturbed horizontal surface. Hence, any analysis starts out with the benefit of a complete set of simple well-known governing equations and a relatively tractable geometry.

Many problems in ocean-wave physics have been solved. Some classical analyses were completed well over a hundred years ago—a mixed blessing for present-day theorists who have to live with a nagging suspicion that their problem has already been solved somewhere.

Other problems have resisted solution. The full set of governing equations is nonlinear and approachable only with strong approximations; waves with slopes of only 20 degrees are strongly nonlinear. If the water motion becomes turbulent, even approximate solutions fail. Turbulence is one of the unsolved puzzles of classical physics.

Still other problems have remained speculative because data on ocean waves are so difficult to obtain. Analyses have had to proceed with only guesses for initial and boundary conditions. The growth of waves due to wind, for instance, has been studied intensively for well over thirty years, and yet there is only one well-documented experiment[1] in which winds and ocean waves were simultaneously measured with sufficient resolution to address salient questions.

The classical foundation of ocean-wave physics thus does not reduce the study to a simple application of known principles. The benefits of such a secure foundation are more subtle. The specific benefit to be explored in this article is that straightforward analysis of simple models can yield significant results.

David E. Irvine is a senior staff physical oceanographer in the Space Geophysics Group, The Johns Hopkins University Applied Physics Laboratory, Laurel, MD 20707.

SIR-B OFF THE SOUTH AFRICAN COAST

Space shuttles have twice flown the Shuttle Imaging Radars (SIRs) into orbit. The second flight, early in October 1984, carried the experiment known as SIR-B. Several results of the experiment are given in other articles in this issue.

The SIR is a synthetic aperture radar (SAR), one of the most powerful microwave remote sensors ever used to study the ocean. Intensive study has shown that under favorable conditions, the SAR can reliably map ocean waves.

During the SIR-B experiment, a strip of SAR images was acquired off the South African coast. Figure 1 indicates the location of these image squares with respect to both the African coast and the local bottom topography. Figure 2 shows a portion of the data in which the images have been divided into squares 6.4 kilometers on a side. Finally, Fig. 3 shows spectra constructed from the image squares in row 2 of Fig. 2. The upper left-hand spectrum is from row 2, column 6; the lower right is from row 2, column 21.

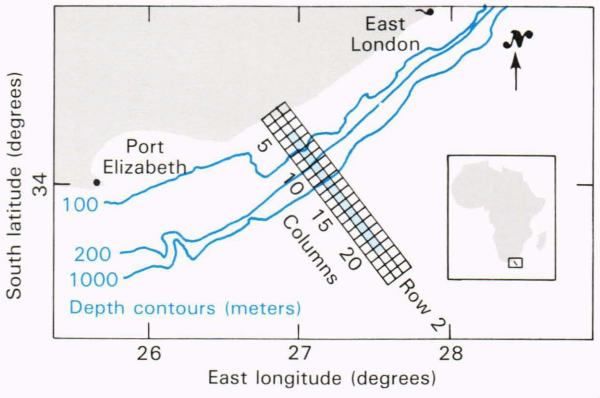

Figure 1—The SAR data were taken off the southeast coast of South Africa, as shown in the insert, about midway between East London and Port Elizabeth. The 6.4-kilometer squares shown here are enlarged in the actual SAR imagery shown in Fig. 2. The spectra calculated from the shaded squares are shown in Fig. 3.

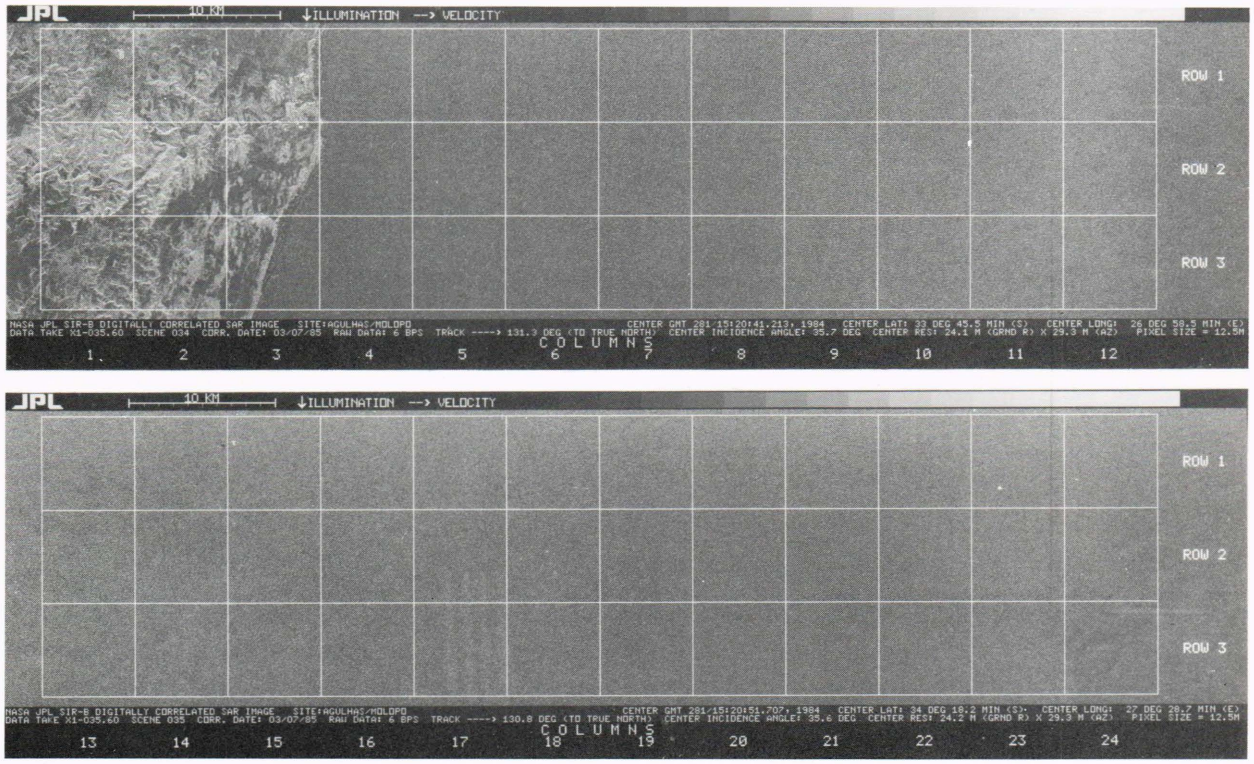

Figure 2—Digitally correlated SAR images from SIR-B. The African coast is on the left. The enhanced wave field in columns 9 to 13 is just visible. The three distinct lines in column 17 are spurious.

Obtaining quantitative ocean-wave spectra from SAR images is an elaborate and still controversial process. Elsewhere in this issue, Monaldo discusses some of the problems. Suffice it to say that we have constructed estimates of ocean-wave slope and height spectra from similar SIR-B images off the coast of Chile with success. With the techniques applied to the South African data set, the results as displayed should represent reasonable estimates of slope spectra.

Examining the spectra, it is evident that two wave systems are present consistently: a swell field from the southwest of approximately 190 meters wavelength and a somewhat longer swell out of the southeast with a wavelength of roughly 220 meters. Additional data from Waverider buoys and synoptic weather charts corroborate this interpretation. Figure 4 shows the present best guess for the directions of these systems.

The dramatic energy intensification in the spectra extracted from the images in columns 9 to 13 of Figs. 1 and 2 is striking. Our immediate goal is to account for this phenomenon.

THE AGULHAS CURRENT

Just off the South African coast is the Agulhas Current. With a mean speed of 2 knots and a mean flux of 20 million metric tons per second, the Agulhas is the third fastest current in the world; only the Gulf Stream and the Kuroshio, off Japan, are faster. The current is approximately 100 kilometers wide and flows southwest along the African coast, swinging seaward south of Port Elizabeth. Near East London, the maximum current is approximately 50 kilometers offshore.

Figure 5 is an infrared image from METEOSAT, a European geostationary weather satellite, taken one day before the data in Fig. 2. The Agulhas is clearly visible as a light-colored band hugging the coast. The current is evidently very close to its average position. There is no indication of a major meander in the current; basically, it looks straight.

The space shuttle image swath crossed the Agulhas at nearly a right angle. Consequently, the shorter wave system, also normal to the flight track, is propagating directly upstream. This opposition to the current is evidently the cause of the increase in spectral intensity of that system.

The next step is to model the interaction of a wave with an opposing current.

WAVE-CURRENT INTERACTION

The physics of swell crossing deep, slowly varying currents was addressed theoretically over 20 years ago.[2] Although direct verification in the ocean has been only approximate, the soundness of the analysis is generally unquestioned. The theory assumes basically two things: first, that the wave field can be adequately characterized by a single wavenumber, κ_0, and second, that the current varies significantly only on scales much greater than $|\kappa_0|^{-1}$.

A further tacit assumption is that the governing equations are nearly linear in wave amplitude. Thus, one can

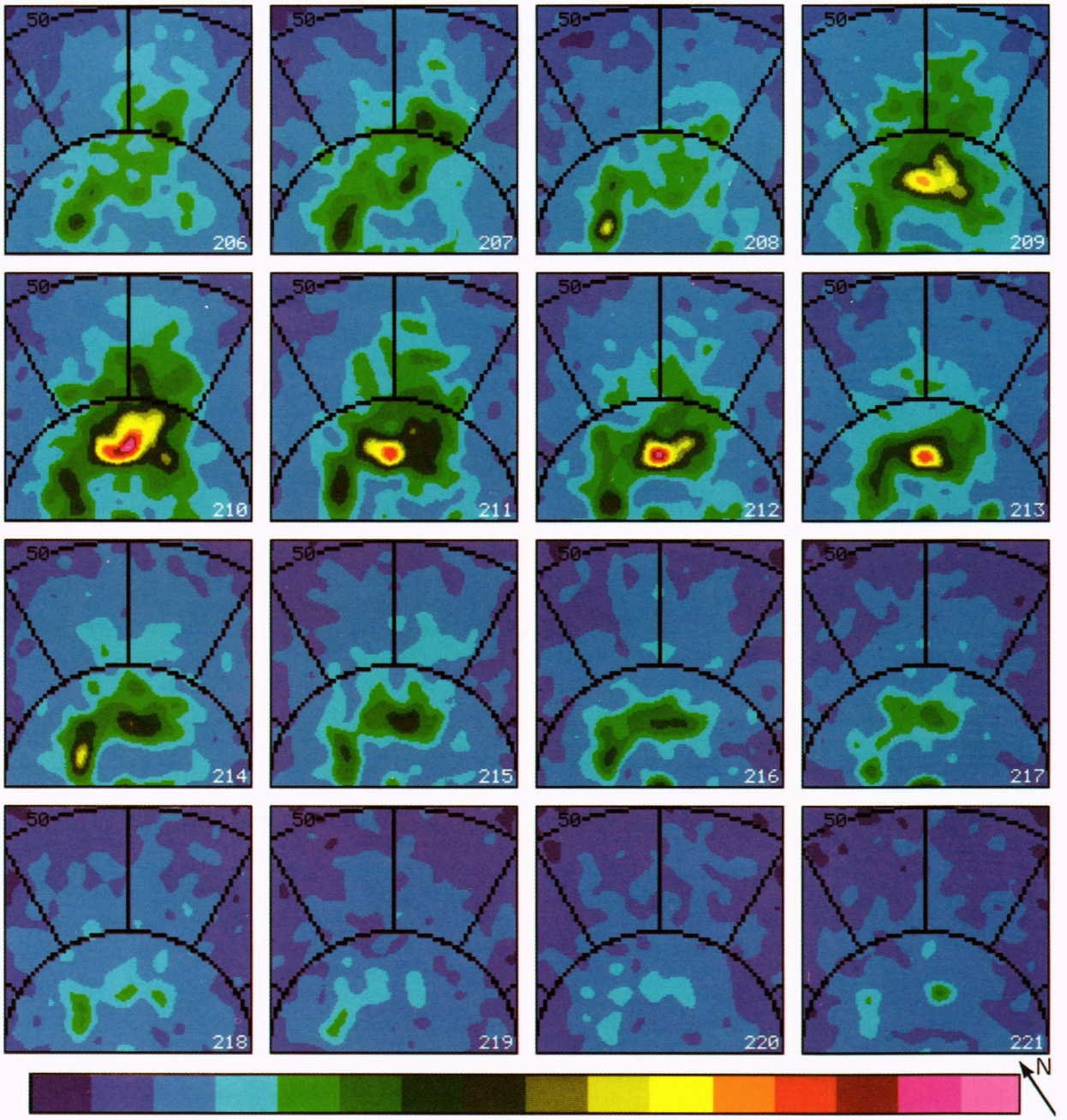

Figure 3—Spectra of image intensity were calculated for each of the 6.4-kilometer squares and then converted to slope spectra; the orientation of these spectra is shown in Fig. 1. All spectra shown are from row 2; the upper left-hand spectrum was computed from column 6, and the lower right, from column 21. The outer circle indicates 50-meter waves, the inner circle, 100-meter waves.

use the linear theory dispersion relation and reasonably associate the frequency, $\sigma_0 = \sqrt{g\kappa_0}$, with the wave ($g$ is the acceleration of gravity).

Figure 6 is an idealized picture of a swell field approaching a current. Seaward of the Agulhas, the wave field is inclined to the upstream direction at an incident angle of ϕ_0. The current itself is modeled as a streamwise-uniform current of arbitrary cross section flowing in the negative x direction, $\mathbf{U} = (-U(y),0)$.

The conservation equations for this model are

$$\frac{\partial}{\partial t}\left(\frac{E}{\sigma}\right) + \nabla \cdot \left[(\mathbf{c}_g + \mathbf{U})\frac{E}{\sigma}\right] = 0\,; \qquad (1)$$

$$\frac{\partial \boldsymbol{\kappa}}{\partial t} + \nabla(\sigma + \boldsymbol{\kappa} \cdot \mathbf{U}) = 0; \qquad (2)$$

$$\nabla \times \boldsymbol{\kappa} = 0\,. \qquad (3)$$

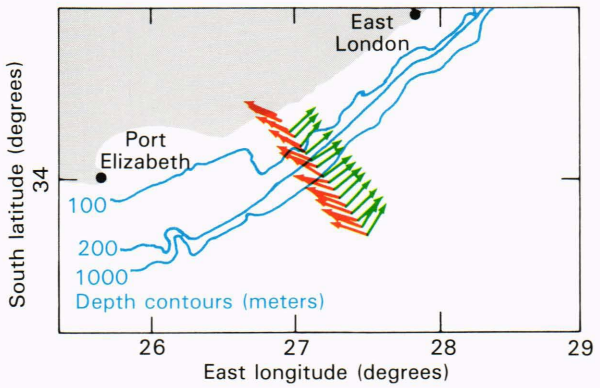

Figure 4—The estimated directions of the two wave systems were taken from the spectral peaks of the two main systems evident in Fig. 3.

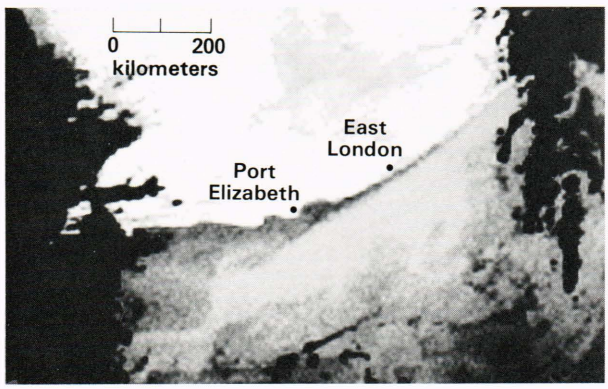

Figure 5—METEOSAT infrared image of the southern tip of Africa, taken one day before the SIR-B data in Fig. 2. The Agulhas is indicated by the warmer and thus brighter band along the coast.

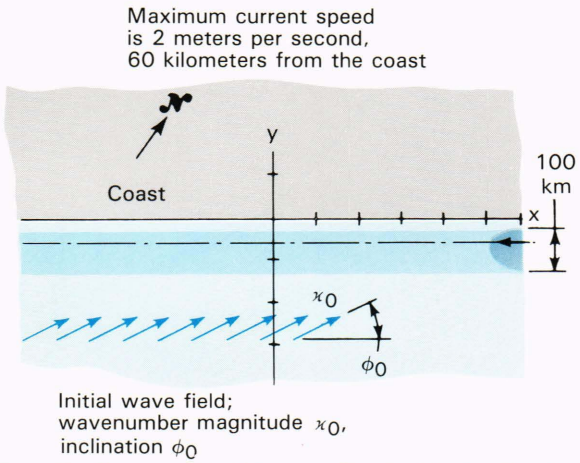

Figure 6—Basic model of the wave field incident on the Agulhas Current.

The energy density, E, is assumed to propagate at approximately the linear theory velocity, $\mathbf{c}_g + \mathbf{U}$, where $\mathbf{c}_g$ is the group velocity. A derivation of this system can be found in Chapter 2 of Ref. 3.

In the few hours required for the wave to cross the stream, the current will vary little; hence, one can assume the variables to be steady. Furthermore, uniformity of both the current and the incident wave field in the x direction allow one to assume negligible x dependence. The conservation laws then reduce to a set of invariants:

$$[c_g \sin(\phi)] \frac{E}{\sigma} = \text{constant}; \tag{4}$$

$$\sigma - \kappa \cos(\phi) U(y) = \text{constant}; \tag{5}$$

$$\kappa \cos(\phi) = \text{constant}. \tag{6}$$

This solution is discussed in Phillips.[4] For a 190-meter system with an incidence angle of $\phi_0 = 10$ degrees, the slope at the maximum current of 2 meters per second would be 26 percent less than seaward of the current. The slope spectra of Fig. 3, however, show a clear increase within the Agulhas. Where is the problem?

THE DOMINANCE OF REFRACTION

The first step toward resolving the discrepancy is to look more closely at the relative role of refraction. The energy density can be represented in terms of an amplitude spectrum:

$$E \sim \int \psi(\boldsymbol{\kappa};\mathbf{x},t)\, d\boldsymbol{\kappa}\,. \tag{7}$$

Equations 2 and 3 indicate that variations in $\boldsymbol{\kappa}$ can be represented as $\boldsymbol{\kappa} = \mathbf{K}(\boldsymbol{\kappa}_{\text{initial}};\mathbf{U}(\mathbf{x}),\mathbf{x},t)$. Thus, the spectral variations are tied to a wavenumber that itself varies. This coupling can be made more explicit by performing the integration over the initial wavenumber range.

$$E \sim \int \psi(\mathbf{K};\mathbf{x},t)\, J(\boldsymbol{\kappa}_{\text{initial}},\mathbf{x},t)\, d\boldsymbol{\kappa}_{\text{initial}}\,. \tag{8}$$

J is the Jacobian of the transformation from $\boldsymbol{\kappa}_{\text{initial}}$ to $\boldsymbol{\kappa}$. This initial wavenumber range is by hypothesis small and centered on $\boldsymbol{\kappa}_0$. Putting this back into the original set of Eqs. 1 to 3 and using Eqs. 2 and 3 to obtain an equation for J, one obtains two invariants where there was only one before (Eq. 4):

$$\frac{\psi}{\sigma} = \text{constant}; \tag{9}$$

$$[c_g \sin(\phi)] J = \text{constant}. \tag{10}$$

Equations 5 and 6, which apply for a spectrum of linearly independent waves as well as for a single monochromatic one, predict that the wavenumber magnitude of a wave incident upstream (ϕ_0 less than 90 degrees) would increase somewhat, as would σ. Thus, ψ would also increase; the spectral density of slope would increase even more.

However, Eqs. 5 and 6 also predict that a wave incident at a small angle would turn dramatically toward the normal. Such refraction can easily be great enough

so that $c_g \sin(\phi)$ increases substantially, forcing J to decrease. Thus the energy density of a wave system may actually decrease in a region where ψ is elevated, which provides us with an important clue.

CURVING CURRENTS—A SMALL DIFFERENCE MAKES A BIG DIFFERENCE

If we look back at Fig. 5, despite the disingenuous comment about the current "basically" looking straight, there is an evident curvature. The radius of curvature is roughly 3500 kilometers; one can perhaps be forgiven for initially disregarding it.

To predict the behavior of a wave field crossing a curving current requires a little more work. First, the kinematic equations, 2 and 3, need to be reformulated into what are known as the ray equations. The details are outlined in the boxed insert.

From the ray equations one can find the trajectories, called rays, taken by a small group of waves. Figure 7 shows the trajectory of a wave incident on a current for two cases. The only difference is the slight curvature of the current in the second case (the bottom panel) which also shows the actual coastline. The qualitative difference is striking; the wave now reflects at the inner boundary. Along that boundary, J becomes very large; the effect of refraction is now to pile up energy along the reflection line.

To determine how much curvature is required to reflect a wave, a sequence of currents was given progressively greater curvatures; for a fixed curvature, the greatest incident angle at which reflection would take place was recorded. Figure 8 shows that exceedingly small curvatures would reflect waves incident at 10 degrees or less. Thus a possible answer to the problem is that the 190-meter swell system may be reflecting along the inner boundary of the Agulhas.

* * *

The subtle benefit of a classical foundation for wave theory is evident here. The extent to which one can realistically manipulate a simple physical model is essentially proportional to the confidence in the basic physics of that model. The model of wave-current interaction represented by Eqs. 1 to 3 is quite secure. The general acceptance of the model by the research community without extensive testing is not an indication of an uncritical attitude; it is a result of the confidence in the model's foundation.

MEANDERS IN THE AGULHAS—A SOURCE OF EXTREME WAVES?

The Agulhas is part of one of the world's most important shipping routes. Oil tankers from the Middle East that are too large for the Suez Canal must sail around Africa to reach Europe or the Americas. The speed of the Agulhas can shorten the time required for the detour. However, the Agulhas is also a fertile breeding ground for what are sometime called "giant waves." It is estimated that such giant waves severely damage or sink a supertanker every year. The time gain is therefore accompanied by a risk.

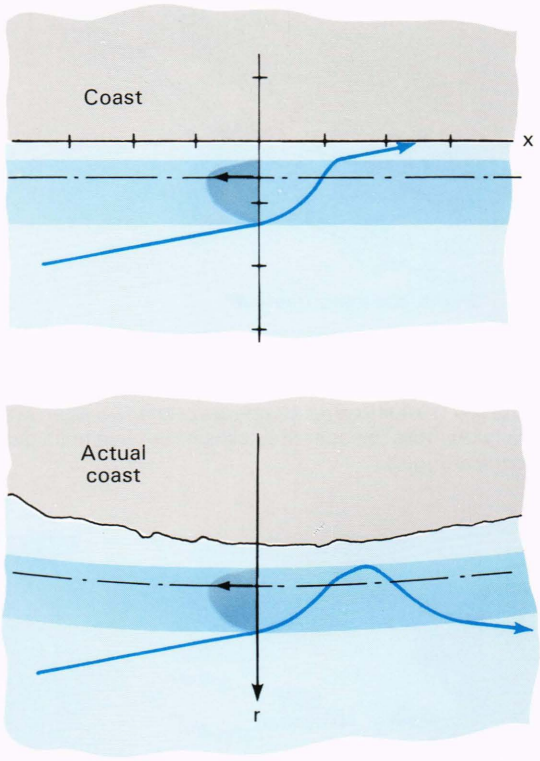

Figure 7—The impact of a slight curvature on the trajectory of a wave group. The top panel shows the trajectory of a wave group crossing a straight current; the bottom panel shows a current with a mild curvature.

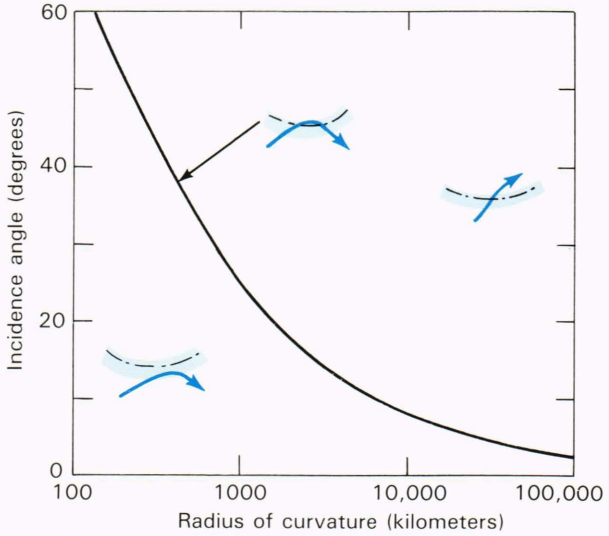

Figure 8—The sensitivity of incident waves to the curvature of a uniformly turning current. The qualitative behavior of the wave in each region is shown (in an exaggerated form).

Data on such waves are understandably rare, but one feature that has been reported is that they seem out of proportion to local conditions. The usual explanation is that random combinations of waves occasionally pro-

THE KINEMATIC WAVE EQUATIONS

The ray equations can be derived from Eqs. 2 and 3 in the text quite simply once they are expressed in terms of Cartesian tensors:

$$\frac{\partial \kappa_i}{\partial t} + \frac{\partial}{\partial x_i}(\sigma + \kappa_j U_j) = 0 \; ; \tag{1}$$

$$\frac{\partial \kappa_2}{\partial x_1} - \frac{\partial \kappa_1}{\partial x_2} = 0 \, . \tag{2}$$

In this notation, the vector **A** is written as the first order tensor A_i. The index i can take on two values, corresponding to two orthogonal directions within the (flat) ocean surface. The scalar product $\mathbf{A}\cdot\mathbf{B}$ is now written A_iB_i, where repeated indexes imply summation. In other words, A_iB_i always means $A_1B_1 + A_2B_2$.

Now begin by expanding the wave conservation equation,

$$\frac{\partial \kappa_i}{\partial t} + (c_g)_j \frac{\partial \kappa_j}{\partial x_i} + \frac{\partial \kappa_j}{\partial x_i} U_j + \kappa_j \frac{\partial U_j}{\partial x_i} = 0 \, , \tag{3}$$

where the group velocity has been introduced:

$$(c_g)_j = \frac{\partial \sigma}{\partial \kappa} \frac{\kappa_j}{\kappa} \, . \tag{4}$$

Using Eq. 2, the ray equation governing wavenumber emerges:

$$\frac{\partial \kappa_i}{\partial t} + [(c_g)_j + U_j] \frac{\partial \kappa_i}{\partial x_j} = -\kappa_j \frac{\partial U_j}{\partial x_i} \, . \tag{5}$$

This can be simplified since the left-hand side of Eq. 5 is just the time derivative observed in a reference frame moving with velocity $(c_g)_j + U_j$. We now have the formal ray equations:

$$\frac{dk_i}{dt} = -\kappa_j \frac{\partial U_j}{\partial x_i} \; ; \tag{6}$$

$$\frac{dR_i}{dt} = (c_g)_i + U_i \; ; \tag{7}$$

where R_i is the location of the wave group. Wave rays are the lines mapped out by R_i.

duce an unusually large wave. This may well be part of the explanation.

Another explanation can be built on an analysis of swell opposing a curving current. The essential element is current meandering. Figure 9, based on an infrared image of the Agulhas taken in 1976,[5] shows a pronounced loop. Evidence suggests that such loops are not uncommon. Based on the analysis above, what would the effect of such a meander be on an incident swell field?

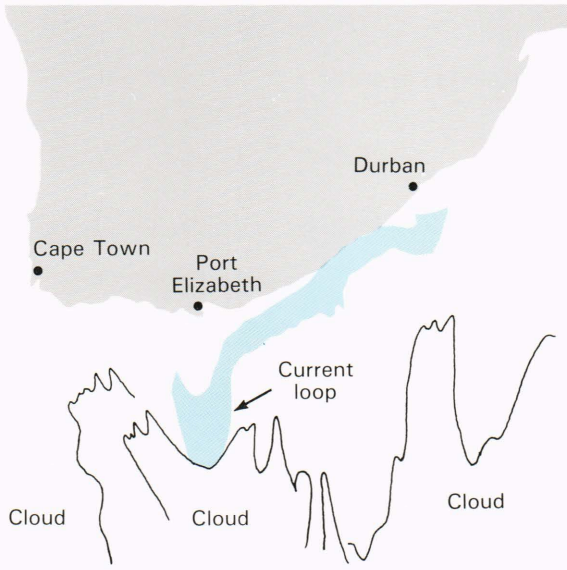

Figure 9—Drawing based on an infrared image of the southern tip of Africa from a National Oceanic and Atmospheric Administration satellite (NOAA-5). A large meander is evident south of Port Elizabeth.[5]

The effect is dramatic. Figure 10 shows two computer simulations of a meander imposed on the same current field used in Fig. 7. A small deflection produces a local focusing of wave rays and thus a local increase in wave energy. A larger deflection adds still another feature: wave trapping. Waves are reflected along much of the upstream side of the meander. Though some energy is reflected back to sea, much energy is trapped within the current. The regions of focused wave rays are very likely to be seen locally as dramatic increases in wave energy.

Thus, giant waves might sometimes be caused by the focusing of swell by meanders in the Agulhas. Such a mechanism would account for the "unexpectedness" of giant waves. The focusing is the net effect of a meander of hundreds of kilometers. The local winds, waves, and currents could otherwise look fairly ordinary. The crew of a ship entering such a focal zone would naturally wonder how such anomalous conditions could arise from such ordinary seas.

This extension of the original analysis is intriguing, but it has one obvious flaw. When rays are closely packed, the assumptions underlying the analysis are violated; when rays cross, the assumptions are violated even more strongly. However, experience with water waves has shown that nonlinear effects frequently do not alter waves so radically that all traces of linear behavior vanish. A linear prediction projected into a nonlinear regime is often a respectable first hypothesis.

* * *

The benefit of a simple, reliable foundation here is plausibility. The clarity of the underlying physics lends a priori strength to the hypothesis. In summary, the usefulness of a simple model is one of the signal benefits of a classical foundation.

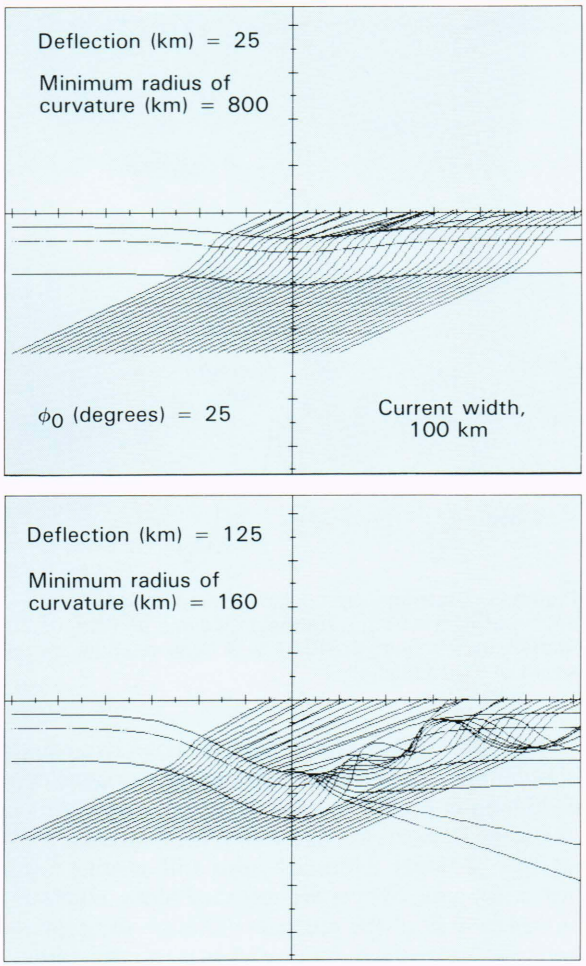

Figure 10—The effect of a meander on a uniform incident wave field. The undisturbed current is identical to that of Figs. 6 and 7. The meander was imposed by first writing that current as a streamfunction: $-U(y) = -\psi_y(y)$. The direction was then perturbed: $\psi(y) \rightarrow \psi(y - f(x))$, where $f(x) = D \exp(x/100\ \text{km})^2$. The maximum deflection, D, is 25 kilometers in the first case and 125 kilometers in the second. The meander in Fig. 9 has a deflection of over 200 kilometers.

THE GROUNDS FOR AN EXPERIMENT

These theoretical conclusions are certainly interesting. But what about the SIR-B data? Are the dramatic increases in wave energy along the northern edge of the Agulhas due to trapped wave energy? The unfortunate answer is that we may never know.

If the waves are very sensitive to small but persistent curvature, then in order to test the theory, those small curvatures must be measured. Ship measurements of the current speeds taken several weeks earlier by Eckart Schumann, a collaborator from the University of Port Elizabeth, were not designed to measure such subtle quantities. The METEOSAT image is likewise inadequate to the task.

The only measurement technique able to measure current fields over an extended area and for an extended time is CODAR, a ground-based radar system. Based on backscattering of dekameter radio waves, CODAR measures currents by the Doppler shifts they induce in the scattered radiation.[6]

SIR-C, the next shuttle-borne SAR experiment, will cross the Agulhas just as SIR-B did. There are tentative plans for CODAR stations to be located along the coast, mapping the current field in sufficient detail to test directly the predictions of a wave-focusing model. And we will be a big step closer to understanding—and, one day, forecasting—extreme waves in the Agulhas.

REFERENCES

[1] R. L. Synder, F. W. Dobson, J. A. Elliot, and R. B. Long, "Array Measurements of Atmospheric Pressure Fluctuations Above Surface Gravity Waves," *J. Fluid Mech.* **102**, 1–59 (1981).

[2] M. S. Longuet-Higgins and R. W. Stewart, "The Changes in Amplitude of Short Gravity Waves on Steady Non-Uniform Currents," *J. Fluid Mech.* **10**, 529–549 (1961).

[3] O. M. Phillips, *The Dynamics of the Upper Ocean*, 2nd ed., Cambridge University Press (1977).

[4] O. M. Phillips, "The Structure of Short Gravity Waves on the Ocean Surface," in *Spaceborne Synthetic Aperture Radar for Oceanography*, R. C. Beal, P. S. DeLeonibus, and I. Katz, eds., The Johns Hopkins University Press, pp. 24–31 (1981).

[5] M. L. Gründlingh, "Observation of a Large Meander in the Agulhas Current," *J. Geophys. Res.*, **84**, 3776–3778 (1979).

[6] F. Dobson, L. Hasse, and R. Davis (eds.), *Air-Sea Interaction: Instruments and Methods*, Plenum Press, New York (1980).

ACKNOWLEDGMENTS—I would like to thank three scientists from South Africa who cooperated in the SIR-B experiment. Frank Shillington, University of Cape Town, provided extensive wave and weather information, as well as interpretations. Eckart Schumann (mentioned above), University of Port Elizabeth, was the principal scientist on a research cruise into the Agulhas two weeks before SIR-B. Finally, Marius Gerber, University of Stellenbosch, worked with me for over a month on the application of wave trapping to the Agulhas extreme wave problem and first suggested the use of CODAR for that problem. I would also like to thank David Tilley of APL for providing me with Fig. 3. This work was supported by the NASA Office of Space Science and Applications.